Fifth Quarterly Progress Report
N01-DC-9-2107

The Neurophysiological Effects of Simulated Auditory Prosthesis Stimulation

C.A. Miller, P.J. Abbas, J.T. Rubinstein, B.K. Robinson

Department of Otolaryngology - Head and Neck Surgery
Department of Speech Pathology and Audiology
Department of Physiology and Biophysics
University of Iowa
Iowa City, IA 52242

January 31, 2001

Contents

1   Introduction

The purpose of this contract is to explore issues involving the transfer of information from implantable auditory prostheses to the central nervous system. Our investigation is being pursued along multiple tracks and include the use of animal experiments and computer model simulations to:

1. Characterize the fundamental spatial and temporal properties of intracochlear stimulation of the auditory nerve.

2. Evaluate the use of novel stimuli and electrode arrays.

3. Evaluate proposed enhancements in animal models of partial degeneration of the auditory nerve.

   In this fifth quarterly progress report (QPR), we focus on the first of these three aims reporting on experiments characterizing the refractory properties of single auditory nerve fibers.

2   Summary of activities in this quarter

In our fifth quarter (1 October - 31 December, 2000), the following activities related to this contract were completed:

1. We attended and presented at the Neural Prosthesis Program Workshop in Bethesda, October 2000. Progress relative to modeling efforts, single fiber measures and developments with respect to the use of multi-electrode arrays to record from the auditory nerve was presented.

2. A manuscript describing measurements of refractory properties was submitted to J. Association for Research in Otolaryngology (see the Appendix). Some of that data is summarized below.

3. More extensive testing of the Michigan CNCT electrode arrays with acoustic stimuli have been conducted. As a consequence of our experience we have worked with personnel at Michigan (J. Hetke) to develop a modified electrode design specific to our needs. Those electrode arrays are now completed and testing will begin in the next quarter.

4. Work continues on the development of a biophysical model that will more accurately simulate properties of auditory nerve fibers as characterized in our physiological data.

3 Response properties of the refractory auditory nerve fiber

3.1 Introduction

From the perspective of information transfer, the refractory property of auditory nerve fibers is a source of distortion, reducing the signal bandwidth that can be encoded by spike timing and introducing a regularity in firing patterns not present in the stimulus. Since cochlear implants generally use modulated pulse trains for stimulation, refractory effects are particularly important in understanding the temporal response patterns under those conditions and consequently the limitations on information transfer. Quantitative measures of refractory properties are also needed to accurately model auditory nerve fiber physiology with computational techniques (e.g., Rubinstein, 1995; Bruce et al., 1999; Mino et al., 2000; Cartee, 2000). Such efforts require not only information on fiber threshold functions, but also how temporal response properties (e.g., latency and jitter) and spike amplitude are altered by refractoriness.

3.2 Methods

Methods of animal preparation and recording are similar to those reported in previous progress reports.

A forward-masking paradigm consisting of a probe pulse preceded by a masking pulse was used to put each measured fiber in a refractory state. Both the masker and probe pulses were monophasic rectangular current pulses of the same polarity separated by a masker-probe interval (MPI). The properties of the masked fiber were assessed at several probe levels (incremented in linear current steps) for several MPI values (ranging from 0.5 to 4 ms).

A number of properties were assessed in analyzing the responses:

1. Action potential amplitude, measured from the spike peak to the subsequent minimum (i.e., the after-hyperpolarization).

2. Mean latency, computed from spike timings across 100 stimulus presentations.

3. Jitter, defined as the standard deviation of spike latencies.

4. Firing efficiency (FE), computed as the percentage of stimuli that evoked an action potential.

5. Threshold, defined as the level yielding an FE of 50%.

6. Relative spread (RS), a measure of the dynamic range of a fiber RS is obtained from a fiber's FE-vs-level function. The FE-vs-level function is fit with a cumulative Gaussian curve and RS is computed as the standard deviation of that function divided by fiber threshold.

Effects of refractoriness were evaluated by plotting threshold, mean latency, jitter, amplitude, and RS as functions of MPI. The first four of these five measures were computed for the 50% FE condition; linear interpolation was typically used to compute those data. For each fiber, the plot of threshold vs. MPI was fit to a decaying exponential function of the form:

$$\theta = \frac{\theta_{SP}}{(1 - e^{(MPI-ARP)/\tau})} \tag{1}$$

where θ, MPI, θ_{SP}, ARP, and τ stand for the fiber threshold, the masker-probe interval (independent variable), the single-pulse (unmasked) threshold, the absolute refractory period, the recovery time constant, respectively.

The fit was performed using the Marquardt-Levenberg algorithm as implemented by Sigmaplot software (version 4; SPSS, Inc.). All three unknown variables on the right side of the equation were allowed to vary during curve fitting, but constrained to positive values. The threshold recovery curves were fit on a fiber-by-fiber basis to provide estimates of τ and ARP.

3.3   Results

Refractory recovery data were obtained from 37 fibers of 7 cats. Of those fibers, 34 responded to cathodic stimuli and 5 responded to anodic stimuli. In 33 of the 37 fibers (89%), cathodic thresholds were lower than anodic thresholds. This is consistent with previously published results showing a strong bias toward lower cathodic thresholds (Miller et al., 1998, 1999). For this reason – and the fact that our small set of anodic data makes it difficult to assess general trends for that stimulus - we have chosen to focus on the data obtained with cathodic stimuli.

Example waveforms are shown in Fig. 1. The top panel shows the "raw" waveforms resulting from 100 repeated presentations of cathodic masker
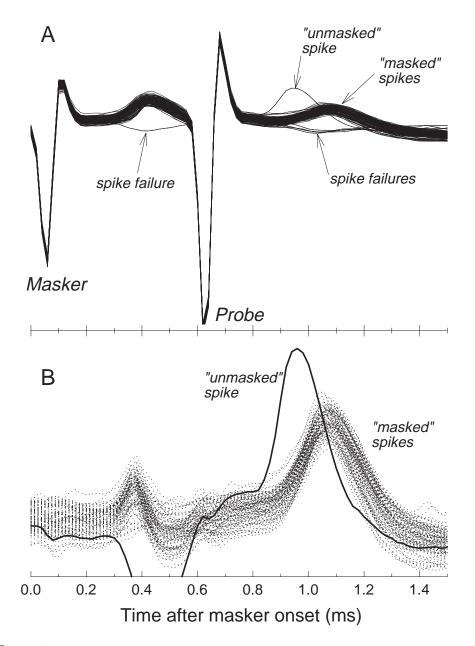
Figure 1: Example of action potentials elicited from a cat auditory nerve fiber under forward-masking conditions. Panel A shows the superimposed responses to 100 presentations of a masker and probe stimulus. Action potentials can be seen in response to both stimuli. Two different responses to the probe are evident. In all but one case, the probe responses were preceded by action potentials to the masker pulse. In the one exception (arrow labeled "spike failure"), the masker failed to elicit an action potential. In that case, the response to the probe has shorter latency and larger amplitude. The amplitude differences between the "unmasked" and "masked" spikes are more clearly seen in panel B, where distortions due to stimulus artifacts and residual EAP have been reduced by means of a template subtraction scheme. Different vertical scales are used in the two panels.

and probe pulses. This data set is particularly illustrative of refractory phenomenon, as, in 1 of the 100 traces, the fiber failed to respond to the masker. In that instance, the probe elicited an "unmasked" spike, which is characterized by shorter latency and greater amplitude than the "masked" spikes. Additionally, the "masked" spikes appear to be somewhat wider than the unmasked spike. These amplitude and morphology effects are more readily seen in the lower panel (B), where a template subtraction method (Miller et al., 1999, 2000) was applied to remove most of the waveform contamination due to the stimulus artifact. Note that in the processed waveforms of panel B, the action potential responses to the masker pulse have been subtracted out. Also, the traces used as the template (i.e., "spike failure" traces in panel A) do not appear in panel B.

Two examples of summary data that were obtained for all fibers are shown in Fig. 2. In the left column, FE, mean latency, and jitter are plotted versus stimulus level for various MPI values. Each of these three functions demonstrates characteristic trends that have been previously reported (Miller et al., 1999). The FE-level functions are well-described by integrated gaussian functions while the latency and jitter functions are, typically, monotonically decreasing functions. From each of these plots, we derived measures of threshold, mean latency (at 50% FE), and jitter (at 50%). These three measures, along with RS and mean spike amplitude (at 50% FE) are plotted for the two fibers in the graphs of the right column of Fig. 2.

Some of the trends produced by these two fibers warrant attention, as they are evident in other fibers of our data set. The threshold-MPI functions of the two fibers of Fig. 2 (right column) fit our model function quite well, as did most fibers. In both exemplar fibers, relative spread was observed to increase with decreasing MPI values and jitter decreased with decreasing MPI. The latency-level functions of fiber C56-4-4 (top panels) reveal a pattern seen in 16 of 34 (47 %) of fibers: increasing latencies with decreasing MPI values. The trend toward longer latencies with smaller MPI values, however, was not consistently observed, as is evident in the data of fiber C46-3-4 (lower panels). In this case, response latencies were smaller for the shorter masker-probe intervals. This trend was observed in 7 of 34 (21 %) of the fibers (either constant or indeterminate latency vs. MPI trends were seen in the other 11 fibers). Both examples of mean action potential amplitude as a function of MPI in the right column show a peak in the function at 1 ms MPI. We note that the 1-ms condition was generally measured near initial contact with the unit and consequently had a larger amplitude. This
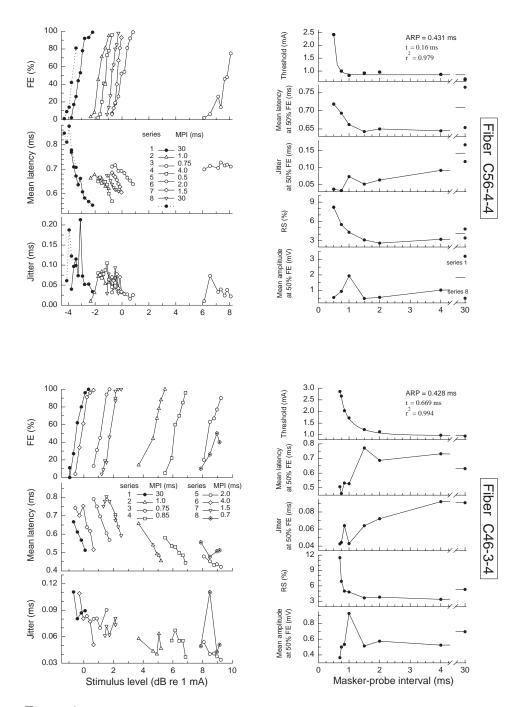
Figure 2: Examples of data obtained for all fibers of this study. Data from two fibers are shown to illustrate the trends encountered across fibers (see text). Input-output plots of the left column show how firing efficiency, mean spike latency, and jitter varied with stimulus level and parametric variation of masker-probe interval. The symbol legend lists the various MPI conditions in the order in which data were collected and the dotted lines in the upper plots indicate a repeated data set. Plots of the right column indicate how spike threshold, mean latency (at 50% FE), jitter (at 50%), relative spread, and spike amplitude (at 50% FE) vary with MPI. In all cases, both masker and probe stimuli were monophasic cathodic pulses delivered by a monopolar intracochlear electrode.

effect is likely due to changes over time rather than MPI. In group analysis, as shown in Figure 3 below, we have corrected for these time related effects.

Estimates of threshold recovery characteristics are presented in Table 1. Included are mean, standard deviation, minimum, and maximum values for the threshold, ARP, and τ estimates, as well as the r^2 values and number of points used to fit each curve. From the pool of 20 fibers analyzed for their fitted recovery curves, the minimum estimated ARP was 139 μs and the maximum ARP was 461 μs.

In addition to estimating threshold recovery parameters, we examined how other single-fiber measures varied as a function of masker-probe interval. We pooled data from all 34 fibers and plotted measures of mean latency, jitter, RS, and amplitude versus MPI. The latency, jitter, and amplitude measures were obtained for the 50 % FE condition. To better discern across-fiber trends, each measure was normalized to the value obtained in the unmasked state. The mean latency and jitter measures were normalized by subtracting the unmasked measures from each fiber's data. The RS and amplitude measures were normalized by dividing each fiber's data by the unmasked measures. Plots of these normalized measures are shown in Fig. 3, along with a plot of normalized threshold vs. MPI. Mean values for each MPI are plotted with open circles.

Table 1:

	Threshold (mA)	ARP (μs)	τ (μs)	r^2	Data points per fiber
Mean	0.768	332	411	0.972	6.1
Standard deviation	0.296	97.9	226	0.0236	1.07
Maximum value	1.30	461	894	0.999	8
Minimum value	0.283	139	131	0.923	4

For each of the five scatter plots of Fig. 3, the data have been fit to functions using the Marquardt-Levenberg algorithm. To describe trends as a function of MPI, we first attempted to fit each data set using hyperbolic, exponential, logarithmic, and rational series, i.e., "plausible" functions that followed a monotonic course and had a horizontal asymptote at large MPI values. If those functions failed to reveal a significant correlation, we expanded the set of functions to include nth-order polynomials. The specific form of each function is shown in each panel of Fig. 3, along with the variance (r^2) explained by each fit. In all but one scatter plot (latency vs. MPI

$$y = 1 / (1 - e^{-(x-x_0)/\tau})$$
$$r^2 = 0.416$$

$$y = mx - y_0$$
$$r^2 = 0.0011$$

$$y = a / (1 + x)^b$$
$$r^2 = 0.128$$

$$y = 1 + Ae^{-(x-x_0)/\tau}$$
$$r^2 = 0.0969$$
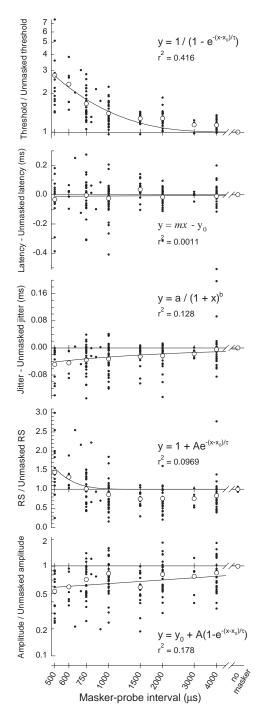
$$y = y_0 + A(1-e^{-(x-x_0)/\tau})$$
$$r^2 = 0.178$$

Figure 3: Five measures (threshold, mean latency, jitter, RS, and amplitude) obtained from all 34 fibers are plotted as a function of MPI. For each of the measures, the data for each fiber was normalized to the value obtained under the no-masking condition. Each scatter plot was fit to a function (the form of which is listed in each panel) in order to assess whether or not each dependent variable was significantly correlated with MPI. These fits are also plotted and the amount of variance explained (r^2) is listed in each panel. Mean values data at specific MPI values are indicated by open circles.

plot), statistically significant functional relationships were found, as determined by the test for correlation between two variables (Bevington, 1969). With the exception of spike latency, all single-fiber measures (threshold, jitter, RS, and amplitude) were dependent upon MPI.

3.4 Summary

We collected data from single auditory nerve fibers of cats that characterize their response properties when stimulated with forward-masked cathodic current pulses. These data provide a fuller understanding of how auditory nerve fibers respond when placed in a refractory state. In contrast to previously published studies, we found that fibers, on average, have relatively short absolute refractory periods (330 μs) as well as relatively short (410 μs) recovery time constants. We also noted that fibers produce reduced-amplitude action potentials in the relative refractory period. They also demonstrate elevated relative spread values during this period, indicating an increase in their stochastic properties. All of these findings are highly relevant to ongoing efforts to develop accurate computational models of the mammalian auditory nerve fiber. These modeling endeavors could significantly advance our understanding of information transfer in the electrically stimulated auditory nerve as well as accelerate the design of better auditory prostheses.

4 Plans for the next quarter

In the sixth quarter, we plan to do the following:

- Test new design of Michigan electrode in auditory nerve and conduct experiments with electrical stimulation.

- Continue to refine model properties to more closely approximate physiological data.

- Expand stimulus set for experiments using analog stimulation and conditioning stimuli (see Fourth Quarterly Progress Report).

5 Appendix: Presentations and publications

The following manuscript was submitted to J. Association for Research in Otolaryngology:

- Miller, C., Abbas, P., Robinson, B. (2000) Assessing refractory properties of the electrically stimulated auditory nerve.

References

[1] Bruce, I.C., Irlicht, L.S., White, M.W., O'Leary, S.J., Dynes, S., Javel, E., Clark, G.M. (1999) A stochastic model of the electrically stimulated auditory nerve: pulse-train response. IEEE Trans. Biomed. Eng. 46, 630-637.

[2] Cartee, L.A. (2000). Evaluations of a model of the cochlear neural membrane. II: Comparison of model and physiological measures of membrane properties measured in response to intrameatal electrical stimulation. Hear. Res. 146, 153-166.

[3] Miller, C. A., Abbas, P. J., Robinson, B. K., Rubinstein, J. T., Matsuoka, A. J. (1999). Electrically evoked single-fiber action potentials from cat: responses to monopolar, monophasic stimulation. Hear. Res. 130, 197-218.

[4] Miller, C.A., Abbas, P.J., Brown, C.J. (2000) An improved method of reducing stimulus artifact in the electrically evoked whole nerve potential. Ear & Hear. 21, 280-290.

[5] Mino, H., Rubinstein, J.T., Miller, C.A., Abbas, P.J. (2000) Fourth Quarterly Progress Report, N01 DC-9-2106 "Effects of remaining hair cells on cochlear implant function".

[6] Rubinstein, J.T. (1995) Threshold fluctuations in an N sodium channel model of the node of Ranvier. Biophys. J. 68, 779-785.